Modelling of the viscoelastic behaviour of amorphous thermoplastic/glass beads composites based on the evaluation of the complex Poisson's ratio of the polymer matrix

Amen Agbossou, Anne Bergeret, Karim Benzarti, N. Alberola

Modelling of the viscoelastic behaviour of amorphous thermoplastic/glass beads composites based on the evaluation of the complex Poisson's ratio of the polymer matrix

A. AGBOSSOU, A. BERGERET, K. BENZARTI, N. ALBEROLA

Laboratoire Matériaux Composites, ESIGEC, Université de Savoie, BP 1104, 73011 Chambery Cedex, France

A series of polystyrene/glass beads composites were studied by using dynamic mechanical spectrometry. From experimental data obtained under isothermal conditions, a simulation method of viscoelastic behaviour of amorphous thermoplastics reinforced by glass beads was devised. Such a theoretical approach confirmed the requirement of considering the Poisson's ratio as a complex component over all the temperature range. This could be related to the difference of many powers of ten between the moduli of the two phases. Thus, we suggest in this paper a method to evaluate the complex Poisson's ratio of the matrix. From these results, the influence of filler content on the magnitude of the mechanical relaxation related to the glass transition is taken into account.

Nomenclature

r, θ, Ψ	Spherical polar coordinates
σ_{ij}	Stress components
U_r, U_θ, U_ψ	Displacement components
λ, G, ν, K, E	Elastic properties: Lamé constant, shear modulus, Poisson's ratio, bulk modulus and Young's modulus, respectively
c, m, i	Subscripts referring, respectively, to composite material, matrix phase, spherical inclusion phase
a	Radius at spherical inclusion to matrix interface
b	Radius at matrix to equivalent homogeneous medium interface
v_i or v	Volume fraction of inclusions
V_L, V_T	Longitudinal and transverse velocities
ρ	Mass density of the material
p	Hydrostatic stress

1. Introduction

The elastic properties of a homogeneous and isotropic material as a composite reinforced by glass beads are usually described by four parameters i.e. Young's modulus, E, the shear modulus, G, the bulk modulus, K, and Poisson's ratio, ν. Only two of these parameters are required for a complete description of the elastic properties of such a material.

A great many investigations have been carried out on two-phase elastic models in order to describe the mechanical behaviour of homogeneous and isotropic materials [1, 2]. Among these two-phase elastic models, three are commonly used:

(i) the variational models which give an upper bound and a lower bound for the elastic moduli by minimizing the strain energy [3–5];

(ii) the self-consistent models which describe the elastic mechanical behaviour of a composite material by applying the adequate boundaries conditions to a single composite sphere embedded in an equivalent homogeneous medium [6, 7];

(iii) the phenomenological models which lead to a description of elastic mechanical behaviour by means of empirical or semi-empirical equations [8, 9].

In order to extend these various elastic models to describe the viscoelastic behaviour of material, Dickie [10] has developed a correspondence principle. This correspondence principle states that the complex moduli of composites may be obtained by substituting phase elastic moduli for phase complex moduli in the previous two-phase elastic models. Thus, in viscoelastic materials, the mechanical properties are time dependent. This time dependence is well known for deformation in shear, G, and in uniaxial elongation, E [11]. For K and ν, some authors assumed that their variations are time (or temperature) independent. With this assumption, experimental and theoretical data are in good agreement for polymer–polymer composites [12, 13]. This could be due to the slight difference between the moduli of the two phases over the time (or temperature) range. However, direct

measurements of K and ν have exhibited a time-dependent behaviour [14–18].

The purpose of the present work was:

(i) to confirm the requirement of using complex components K^* and ν^* of each phase, especially when the moduli of the two phases remain very different over the time (or temperature) range;

(ii) to suggest a method to determine the complex bulk modulus, K^*, and the complex Poisson's ratio, ν^*, of the polymer used as matrix versus temperature (or time);

(iii) to simulate the viscoelastic behaviour of amorphous thermoplastics reinforced by glass beads and compare theoretical data to experimental results.

2. Experimental procedure

2.1. Materials

Composites specimens are based on polystyrene reinforced by 6%–50% volume fraction of glass beads. Polystyrene ($\bar{M}_n = 99\,500$, $\bar{M}_w = 306\,800$) was provided by Orkem Company; glass beads were supplied by Microbeads Company. Two different size distributions of particles were used: the first over the range 1–45 μm and the second over the range 70–110 μm. These glass beads were dried in an oven at 100 °C and no particular treatment was performed on them. The volume fraction of particles was determined by burning composites samples at 600 °C for 45 min.

The composite was extruded at 200 °C. This extrusion was carried out in a twin-screw extruder from Leibtritz (LSM 30–34). Then the extrudate samples of varying volume fraction were moulded at 200 °C under high pressure (200 bar) and cooled at room temperature. In order to give the same thermal history to each sample, specimens were heated at temperatures higher than their glass temperature and then cooled to room temperature at the same cooling rate. The moulded samples were finally cut for experimental work to the following dimensions: 20 mm × 4 mm × 5 mm for dynamic mechanical analysis and ultrasonic measurements. The surfaces of specimens were flat and parallel to one another.

2.2. Dynamic mechanical spectrometry

Dynamic mechanical spectrometry was carried out using a Viscoanalyser (Metravib Company, France). This apparatus provides the real, E', and imaginary, E'', parts of the dynamic stress modulus and the internal friction $\tan\phi (= E''/E')$ as a function of the temperature (for one or several frequencies) or of the frequency (under isothermal conditions).

Thus, frequency scans were performed by increasing the temperature from 30 °C to 200 °C at several frequencies over the range from 5–100 Hz. Several measurements were repeated for both frequency and temperature scans in order to verify that no physical ageing occurred in materials during experiments.

2.3. Ultrasonic experimental technique

In order to characterize our materials, we used the standard ultrasonic technique which measures the time-of-flight of a wave crossing the material. The wave pulse is established at one surface of the sample by a transmitting transducer. The transmitting receiver is shut down for a short time so that it can receive the reflected signal from the surface. The distance travelled by the pulse is known, and the time-of-flight is measured by timing the signal on its travel through the specimen, so one can calculate the velocity of propagation of the ultrasonic wave. In isotropic materials, the velocities determined by this method are used to calculate the material moduli. Two independent velocities (longitudinal velocity, V_L, and transverse velocity, V_T) measurements are required to determine the complete elastic moduli of the isotropic material. From these two velocity values, one can calculate the Lamé constant, λ, and the shear modulus, G, using the following relations

$$V_L = \left(\lambda + 2\frac{G}{\rho}\right)^{1/2} = \left[\frac{E(1-\nu)}{\rho(1-2\nu)(1+\nu)}\right]^{1/2} \quad (1)$$

$$V_T = \left(\frac{G}{\rho}\right)^{1/2} = \left(\frac{E}{2\rho(1+\nu)}\right)^{1/2} \quad (2)$$

where ρ is the mass density of the material.

3. Results

3.1. Ultrasonic elastic constant measurements

From the calculation of λ and G, Young's modulus, E, and Poisson's ratio, ν, can be determined. Table I gives the ultrasonic elastic constants at room temperature of polystyrene matrix.

3.2. Dynamic mechanical spectrometry

3.2.1. Polystyrene matrix

Plots of log E' and tan ϕ of a polystyrene matrix at five frequencies, i.e. 5, 10.5, 22.3, 47.2 and 100 Hz, versus temperature are shown in Fig. 1. The tan ϕ maxima and log E' plots related to the glass transition show a frequency dependence. It can be observed that the time–temperature dependence does not follow an Arrhenian law over the temperature range. In fact, it is well known that the relaxation related to the glass transition is not a thermorheologically simple process and is of WLF type [11].

TABLE I Ultrasonic elastic constants at room temperature of polystyrene matrix ($\rho = 1.0535\ \mathrm{kg\,m^{-3}}$)

V_L ($\mathrm{m\,s^{-1}}$)	V_T ($\mathrm{m\,s^{-1}}$)	λ (10^9 Pa)	G (10^9 Pa)	E (10^9 Pa)	ν
2295	1146	2.78	1.38	3.69	0.33

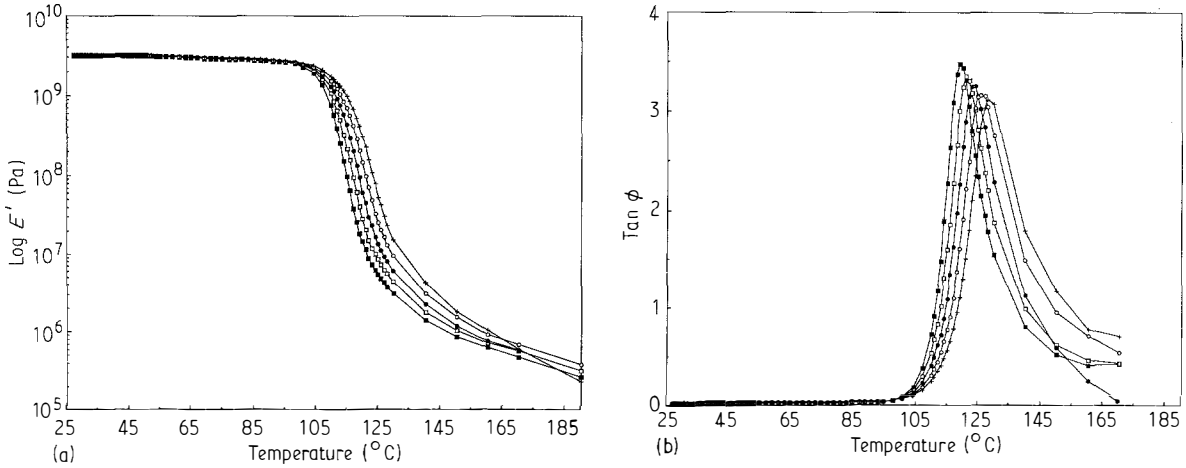

Figure 1 Plots of (a) log E', and (b) tan ϕ versus temperature for polystyrene matrix for various frequencies: (■) 5 Hz, (□) 10.5 Hz, (●) 22.3 Hz, (○) 47.2 Hz and (+) 100 Hz.

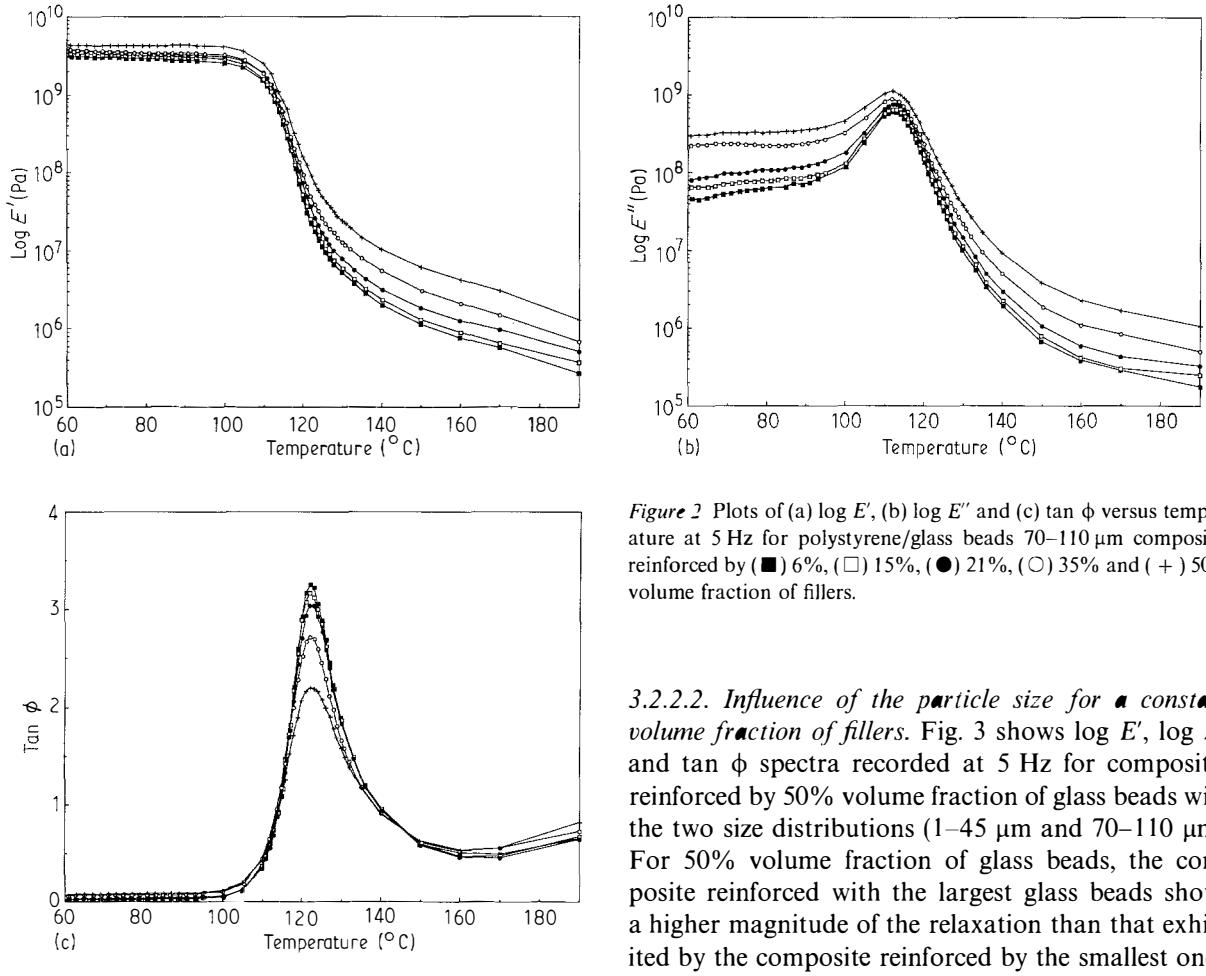

Figure 2 Plots of (a) log E', (b) log E'' and (c) tan ϕ versus temperature at 5 Hz for polystyrene/glass beads 70–110 μm composites reinforced by (■) 6%, (□) 15%, (●) 21%, (○) 35% and (+) 50% volume fraction of fillers.

3.2.2. Composite materials

3.2.2.1. Influence of the volume fraction of glass beads. Fig. 2 shows log E', log E'' and tan ϕ spectra recorded at 5 Hz for composites reinforced by 6%, 15%, 21%, 35% and 50% volume fractions of fillers with the size distribution 70–110 μm. With increasing volume fraction of fillers, the magnitude of the mechanical relaxation is decreased and the tan ϕ maximum is shifted towards higher temperatures. The vitreous modulus is slightly increased while the rubbery modulus is enhanced with increasing filler content.

3.2.2.2. Influence of the particle size for a constant volume fraction of fillers. Fig. 3 shows log E', log E'' and tan ϕ spectra recorded at 5 Hz for composites reinforced by 50% volume fraction of glass beads with the two size distributions (1–45 μm and 70–110 μm). For 50% volume fraction of glass beads, the composite reinforced with the largest glass beads shows a higher magnitude of the relaxation than that exhibited by the composite reinforced by the smallest ones. Thus, for similar volume fraction of fillers, it can be observed that the reinforcement effect increases with decreasing average size of glass beads. Then, for similar volume fraction of fillers, the specific surface of the glass beads increases as their average size decreases. It can be concluded that the interface related to the specific surface of the glass beads could influence the dynamic mechanical behaviour of composite materials. Thus, it can be suggested that the interface in such composite materials could tend to decrease the molecular motion ability of the matrix and the interface contribution appears to be greater in composites reinforced with the smallest glass beads.

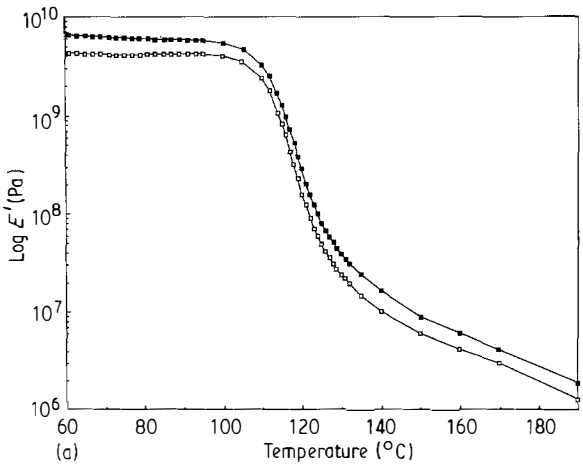

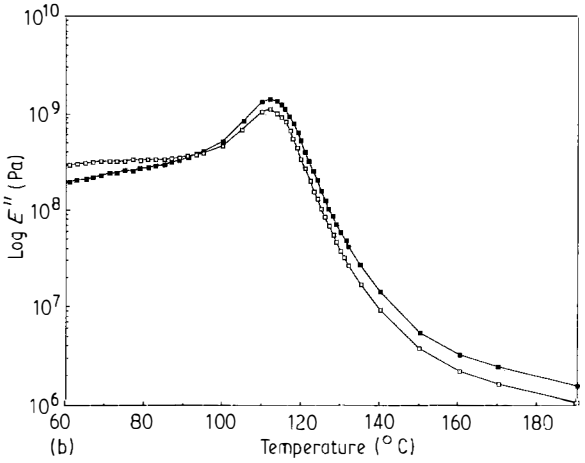

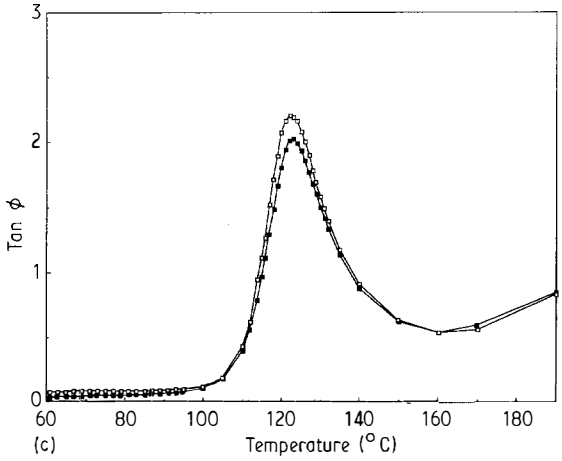

Figure 3 Plots of (a) log E', (b) log E'' and (c) tan ϕ versus temperature at 5 Hz for (■) polystyrene/glass beads 1–45 μm composites reinforced by 50% volume fraction of fillers, and for (□) polystyrene/glass beads 70–100 μm composites reinforced by 50% volume fraction of fillers.

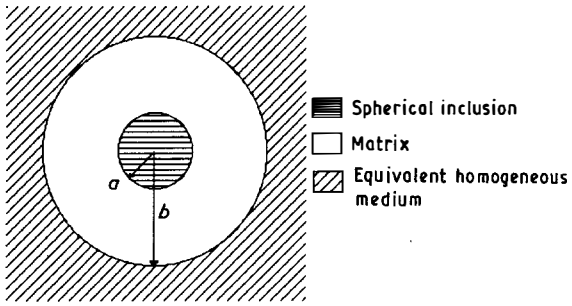

Figure 4 Kerner's and Christensen and Lo's models: a single composite sphere embedded in an equivalent homogeneous medium model.

4. Mechanical models

Among the various two-phase models extended to the viscoelastic behaviour description of composites, Kerner's [6] and Christensen and Lo's [19] approaches were chosen. In fact, these two models give the best agreement between experimental and theoretical data. Kerner's and Christensen and Lo's models provide, respectively, bulk modulus, K, and shear modulus, G. Using Dickie's correspondence principle [10] and the well known elastic relationships, the complex Young's modulus, E^*, and also the complex Poisson's ratio, ν^*, can be calculated from the following relations

$$E^* = \frac{9G^*K^*}{G^* + 3K^*} \tag{3}$$

$$\nu^* = \frac{3K^* - 2G^*}{2(G^* + 3K^*)} \tag{4}$$

4.1. Kerner's model [6]

In order to calculate the effective bulk modulus, Kerner proposed a geometric model of the composite material. This model consists of the single composite sphere embedded in the infinite medium of unknown effective properties (Fig. 4). This model required that the effective homogeneous medium has the same average conditions of stress and strain as does the spherical model of Fig. 4. The homogeneous material sphere is subjected to a hydrostatic stress, p, on its outer boundary. This can be expressed by $\sigma_{rr} = p$, at $r = b$. By means of the average elastic problem analysis, Kerner set the radial displacements as $U_{ri} = A_i r$ and $U_{rm} = A_m r + B_m/r^2$, where the subscripts i and m refer to inclusion and matrix, respectively. The corresponding stresses are found to be

$$\sigma_{rri} = (3\lambda_i + 2G_i)A_i \tag{5}$$

$$\sigma_{rrm} = (3\lambda_m + 2G_m)A_m - 4G_m\frac{B_m}{r^3} \tag{6}$$

The three constants of integration, A_i, A_m and B_m, are evaluated from the continuity conditions on displacements and traction stresses at the interfaces. The calculation of the effective bulk modulus, K_c, of the homogeneous sphere, leads to the following relations

$$K_c = K_m + v_i(K_i - K_m)/[1 + (1 - v_i)\{(K_i - K_m)/(K_m + \tfrac{4}{3}G_m)\}] \tag{7}$$

where $v_i = (a/b)^3$ is the volume fraction of inclusions.

Previous workers [2, 7, 19] have shown that this approach leads to an exact solution for the effective bulk modulus of a homogeneous and isotropic composite material.

4.2. Christensen and Lo's model [19]

Christensen and Lo determined the effective shear modulus based on the same geometric model as Kerner (Fig. 4). By means of the shear deformation equations of a homogeneous medium in simple shear deformation, Christensen and Lo assumed a general displacement for the heterogeneous problem in the form

$$U_r = U_r(r) \sin^2\theta \cos 2\psi \quad (8a)$$

$$U_\theta = U_\theta(r) \sin\theta \cos\theta \cos 2\psi \quad (8b)$$

$$U_\psi = U_\psi(r) \sin\theta \sin 2\psi \quad (8c)$$

where $U_r(r)$, $U_\theta(r)$ and $U_\psi(r)$ are unknown functions of r to be solved from the equilibrium equations. It is interesting to note that the form in Equation 8a–c is consistent with the basic state of shear deformation.

After some calculations, the equilibrium equations lead to:

(i) in the equivalent homogeneous medium ($r \geqslant b$)

$$U_{re} = D_1 r + \frac{3D_3}{r^4} + \frac{(5 - 4\nu)}{(1 - 2\nu)} \frac{D_4}{r^2} \quad (9a)$$

$$U_{\theta e} = D_1 r - \frac{2D_3}{r^4} + \frac{2D_4}{r^2} \quad (9b)$$

(ii) in the matrix phase ($a \leqslant r \leqslant b$)

$$U_{rm} = B_1 r - \frac{6\nu_m}{(1 - 2\nu_m)} B_2 r^3 + \frac{3B_3}{r^4} + \frac{(5 - 4\nu_m)}{(1 - 2\nu_m)} \frac{B_4}{r^2} \quad (10a)$$

$$U_{\theta m} = B_1 r - \frac{(7 - 4\nu_m)}{(1 - 2\nu_m)} B_2 r^3 - \frac{2B_3}{r^4} + \frac{2B_4}{r^2} \quad (10b)$$

and (iii) in the inclusion phase ($0 \leqslant r \leqslant a$)

$$U_{ri} = A_1 r - \frac{6\nu_i}{(1 - 2\nu_i)} A_2 r^3 \quad (11a)$$

$$U_{\theta i} = A_1 r - \frac{(7 - 4\nu_i)}{(1 - 2\nu_i)} A_2 r^3 \quad (11b)$$

where ν, ν_i and ν_m are values of Poisson's ratio. The nine constants (A_1, A_2, B_1, B_2, B_3, B_4, D_1, D_2, D_3) are determined from the continuity conditions at the two interfaces. These conditions involve the continuity of the stresses σ_{rr}, $\sigma_{r\theta}$, $\sigma_{r\psi}$ and the displacements U_r, U_θ and U_ψ. Only eight conditions result from the initial twelve continuity equations due to the redundancy of many of the forms. The continuity conditions give the equations with all other effective properties of the equivalent homogeneous medium such as λ, ν and G.

In order to determine the effective shear modulus, G, by suppressing in the continuity equations all other effective properties such as λ and ν of the equivalent homogeneous medium, Christensen and Lo have used a basic result obtained by Eshelby [20], i.e. for a homogeneous medium containing an inclusion, the strain energy, under applied displacement conditions, is determined by

$$U = U_0 - \frac{1}{2}\int_S (T_i^0 U_{ie} - T_{ie}^0 U_i^0) dS \quad (12)$$

where S is the surface of the inclusion, U_0 is the strain energy in the same medium when it contains no inclusion, T_i^0 and U_i^0 are, respectively, the tractions and displacements in the medium when it contains no inclusion and T_{ie} and U_{ie} are the corresponding quantities at the same point in the medium when it does contain the inclusion.

The final solution for G is given by the solution of the quadratic equation

$$A\left(\frac{G}{G_m}\right)^2 + 2B\left(\frac{G}{G_m}\right) + C = 0 \quad (13)$$

The expressions for coefficients A, B and C are given in the Appendix.

Using the quadratic Equation 13, the exact solution for the equivalent shear modulus of the spherical model can be determined.

4.3 Numerical results and discussion

4.3.1. The Poisson's ratio of the matrix ν_m assumed to be real and constant over the analysed temperature range

We attempt first to determine theoretically the composite dynamic mechanical behaviour knowing the properties of the polymer used as matrix and of the inclusions. The inclusions have elastic behaviour and a constant Young's modulus of 73 GPa over the analysed temperature range. The Poisson's ratio, ν_i, of such fillers is 0.2. In a first approximation, the Poisson's ratio, ν_m, of the matrix is assumed to be real and constant over the temperature range for the numerical simulation ($\nu'_m = \nu_m$; $\nu''_m = 0$). Numerical results were carried out by developing a program computed with Fortran 2.4 language on Macintosh II Ci.

Fig. 5 shows simulated log E' (Fig. 5a), log E'' (Fig. 5b) and tan ϕ (Fig. 5c) curves for composites reinforced by 6% and 50% volume fractions of fillers for a given frequency of 5 Hz. For these simulations, the Poisson's ratio of the matrix is assumed to be a constant and real equal to 0.33 (see ultrasonic measurements). The experimental spectra are also plotted in this Figure.

Fig. 6 shows simulated log E' (Fig. 6a), log E'' (Fig. 6b) and tan ϕ (Fig. 6c) curves for composites reinforced by 50% volume fractions of glass beads at 5 Hz for various real values (from 0.33–0.499) of the Poisson's ratio of the matrix.

As shown in Fig. 5 the magnitude of the experimental relaxation of the composite is significantly reduced by the addition of the glass beads. However, the numerical results obtained by using Kerner's and Christensen and Lo's models show no significant influence of volume fraction of fillers on the internal friction coefficient tan ϕ. The effect of increasing the amount of inclusions on the magnitude of the relaxation is not taken into account by the numerical simulation. This paradox could be related first to the fact that the Poisson's ratio of the matrix is assumed

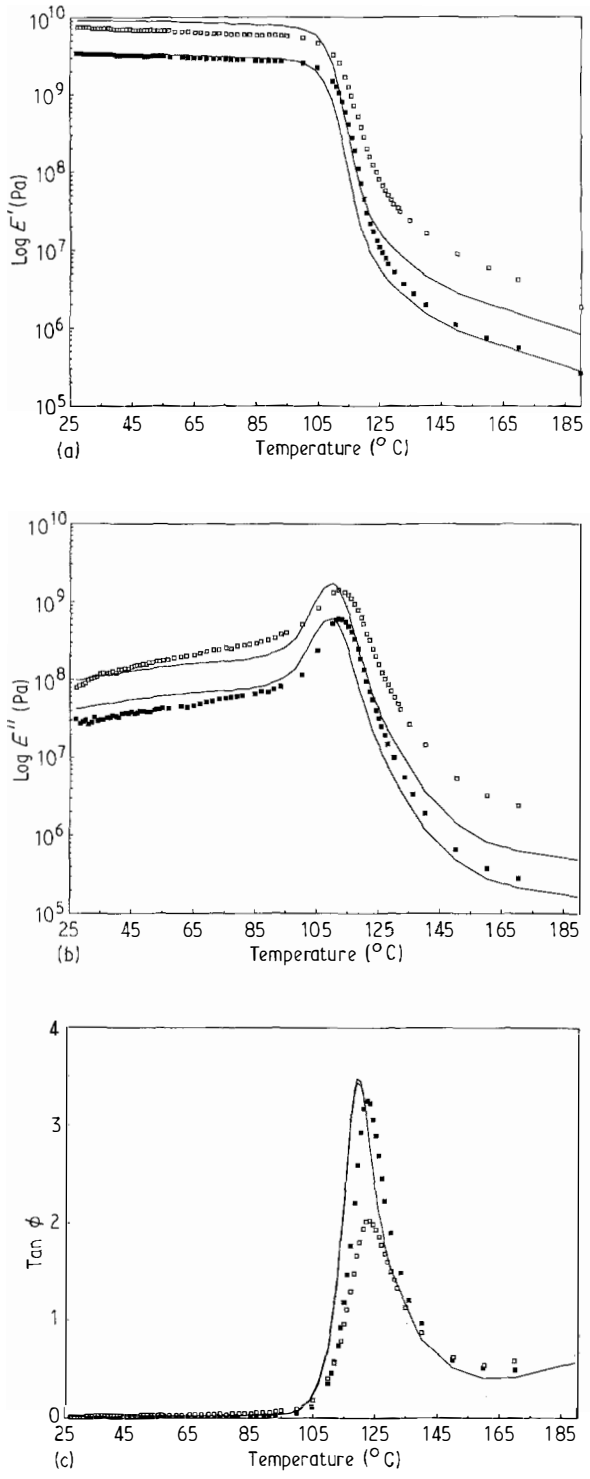

Figure 5 (■, □) Experimental and (——) theoretical plots of (a) log E', (b) log E'' and (c) tan ϕ for polystyrene/glass beads composites reinforced by (■) 6% and (□) 50% volume fraction of fillers.

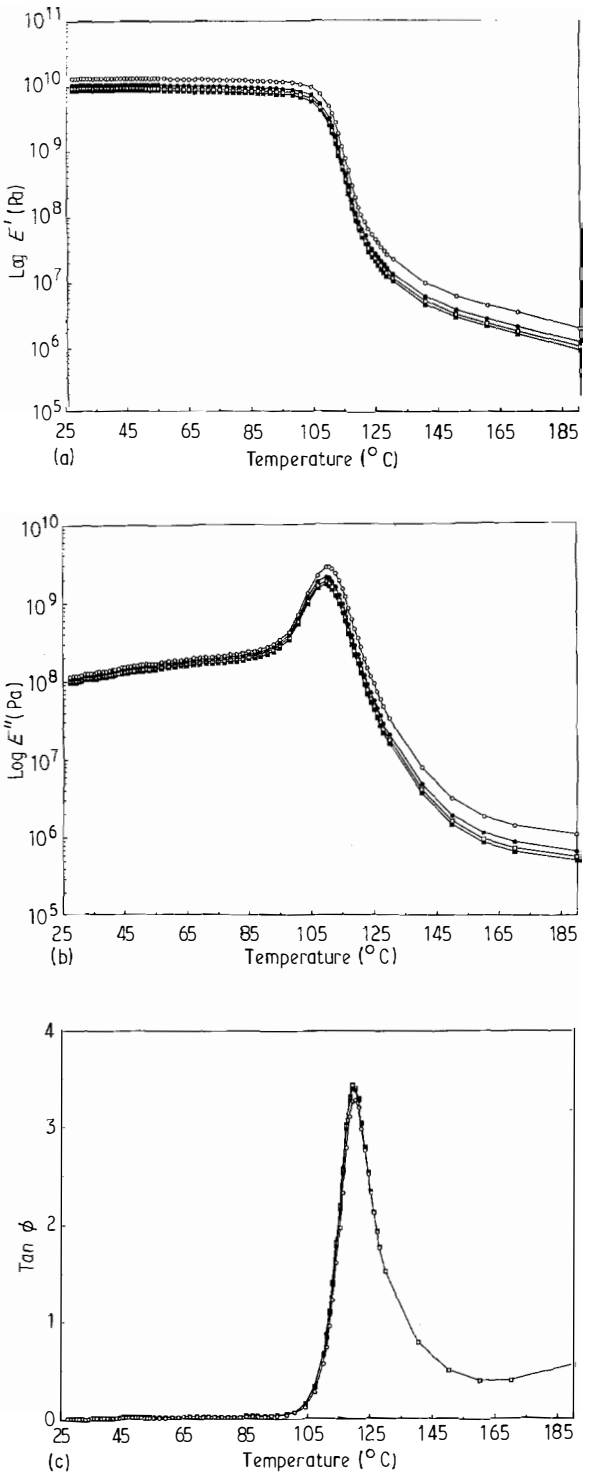

Figure 6 (■, □, ●, ○) Experimental and (——) theoretical plots of (a) log E', (b) log E'' and (c) tan ϕ for polystyrene/glass beads composites reinforced by 50% volume fraction of fillers for various real values of the matrix Poisson's ratio: (■) 0.33, (□) 0.40, (●) 0.45 and (○) 0.499.

to be real and constant over the analysed temperature range and secondly to the fact that the moduli of the two phases remain very different over all this temperature range. Moreover, the shift towards higher temperatures of the tan ϕ peak exhibited by experimental tan ϕ spectra with increasing the filler content, is not revealed by theoretical curves. Furthermore, Fig. 6 shows that, for a given content in inclusions, the real and constant values of ν_m have no influence on the maximum of tan ϕ. All these results lead us to consider ν_m as a complex parameter which is time and temperature dependent. Thus, in order to apply Dickie's correspondence principle to all mechanical parameters, a method to evaluate the complex Poisson's ratio of the matrix $\nu_m^*(=\nu'_m - i\nu''_m)$ is proposed in this paper.

4.3.2. The determination of complex Poisson's ratio of a polymer matrix

The previous simulation suggested the requirement of using complex Poisson's ratio for the polymer matrix,

ν^*. However, the challenge is to determine the behaviour of ν^* over a large temperature range. Several workers have studied this problem by numerical and experimental analyses. The results obtained are sometimes controversial. Two experimental techniques are commonly used: (i) mechanical technique, and (ii) ultrasonic technique.

Some authors have reported Poisson's ratio values obtained by using original methods based on mechanical measurements [14, 21–23]. However, some discrepancies are shown by the use of direct and indirect methods of Poisson's ratio evaluation. For instance, Heydemann [21] has observed that, for polyvinylchloride, ν'_{EG} calculated from E^* and G^*, runs through a minimum, while a direct measurement of this parameter did not show such an evolution versus temperature. These discrepancies between theoretical and experimental data could be related to different (i) samples, (ii) sample thermal histories, (iii) measurement frequencies, and (iv) strain levels. Furthermore, as Young's and shear moduli measurements display small uncertainties, the derivation of Poisson's ratio from these parameters measured separately leads to great uncertainties in the value of ν. Moreover, Heydemann found that the minimum in ν'_{EG} can disappear if the specimen reaches equilibrium at each temperature very slowly. Thus the shape of Poisson's ratio curve depends on the rate of temperature change during the measurements.

But most of the complex elastic constant values were obtained by means of ultrasonic techniques. Some interesting results using this techniques were reported by Waterman and Kono.

Waterman [15–17] used an ultrasonic pulse method to measure the velocity and attenuation of longitudinal and transverse waves of some polyethylenes. In this work the main interest was in the γ transition, which is a secondary transition occurring at temperatures below the main glass transition. From the measured data the complex elastic moduli E^*, G^*, K^* and ν^* were calculated. According to Waterman, a monotonic increase in ν' from about 0.30 to 0.45, accompanied by a maximum in ν'' ($0 < \nu'' < 2 \times 10^{-2}$), was observed in the transition region.

Kono [18, 24] found that for polyvinylchloride and polymethylmethacrylate, the apparent activation energy of the main relaxation in bulk was greater than that in shear. Then, it was suggested that molecular mechanisms involved in the two types of deformation could be different in character.

For polystyrene, Kono [18] has shown that the storage bulk compliance falls from a low-frequency limiting value to a high-frequency limiting value in the glass transition, but this change is less than a factor of two instead of many powers of ten displayed by the shear compliance. In this work Kono found that ν' increases continuously from 0.35 to 0.5 in the glass transition zone.

The technique of evaluation of complex matrix Poisson's ratio, ν^*_m, suggested here rests on the fact that bulk modulus, K^* is a slowly varying function of temperature and time. This assumption agrees with Crowson and Arridge's work [25]. Thus, if the values of $E^*_m(0)$ and $\nu^*_m(0)$ are known at some starting point on the temperature, T, or time t, scale, it is possible to approximate either $\nu^*_m(T)$ or $\nu^*_m(t)$ in a small interval of temperature or time adjacent to this point by

$$K^*_m(T) = K^*_m(0) \rightarrow \nu^*_m(T) = \frac{1}{2}\left\{1 - 2[\nu^*_m(0)] \times \frac{E^*_m(T)}{E^*_m(0)}\right\} \quad \text{for } T \in [0, \delta T] \tag{14}$$

The experimental value of complex matrix Young's modulus, $E^*_m(T)$, and the value of $\nu^*_m(T)$ calculated from Equation 14 are then used for the next temperature interval. The values of Poisson's ratio are alternately calculated for the different temperature ranges. Thus, from a knowledge of experimental $E^*_m(T)$ and one single value of Poisson's ratio, $\nu^*_m(0)$, at the starting point, the complete set of viscoelastic $\nu^*_m(T)$ functions can be displayed.

Fig. 7 shows $\nu_m (= [(\nu'_m)^2 + (\nu''_m)^2]^{1/2})$ (Fig. 7a), ν'_m (Fig. 7b) and ν''_m (Fig. 7c) variations versus temperature at 5 Hz for the polystyrene matrix. These data are in good agreement with Kono's results [16] for polystyrene. As shown in Fig. 7, the real part of the complex Poisson's ratio, ν'_m, of polystyrene increases continuously with temperature as a compliance. The imaginary part, ν''_m, goes through a maximum in the transition region. The variation of tan $\nu_m (= \nu''_m/\nu'_m)$ with temperature is reported in Fig. 7d.

Using the two models described above and using this method of evaluation of the complex Poisson's ratio of the polymer matrix, the dynamic mechanical behaviour of composites can be determined. Fig. 8 shows theoretical and experimental tan ϕ spectra for a composite reinforced by 50% volume fraction of fillers. The influence of filler content on the magnitude of the mechanical relaxation is now taken into account by the numerical simulation, which was not the case considering the Poisson's ratio of the matrix as a real. But, some differences between experimental and theoretical tan ϕ spectra remains. Thus, the theoretical tan ϕ maximum is higher than the experimental tan ϕ peak exhibited by the composite, but significantly lower than those shown by the matrix. These differences in the magnitude of the relaxation between experience and simulation for the composite could be due to some "interface effects" between fillers and matrix. In fact, the magnitude of the relaxation could be related to molecular motion ability of the macromolecular chains. Then, it can be suggested that the occurrence of additional interactions between fillers and chains in a composite could reduce the molecular mobility of the macromolecules. Such a mechanical model could allow the separation of the mechanical behaviour of the two phases in the composite. The properties of the thus-separated matrix could be different from those of the non-reinforced polymer. By using a molecular model of deformation near T_g [26, 27], the molecular motion ability of the separated matrix could be quantitatively compared to those shown by the unfilled polymer. This approach will be developed in a subsequent paper.

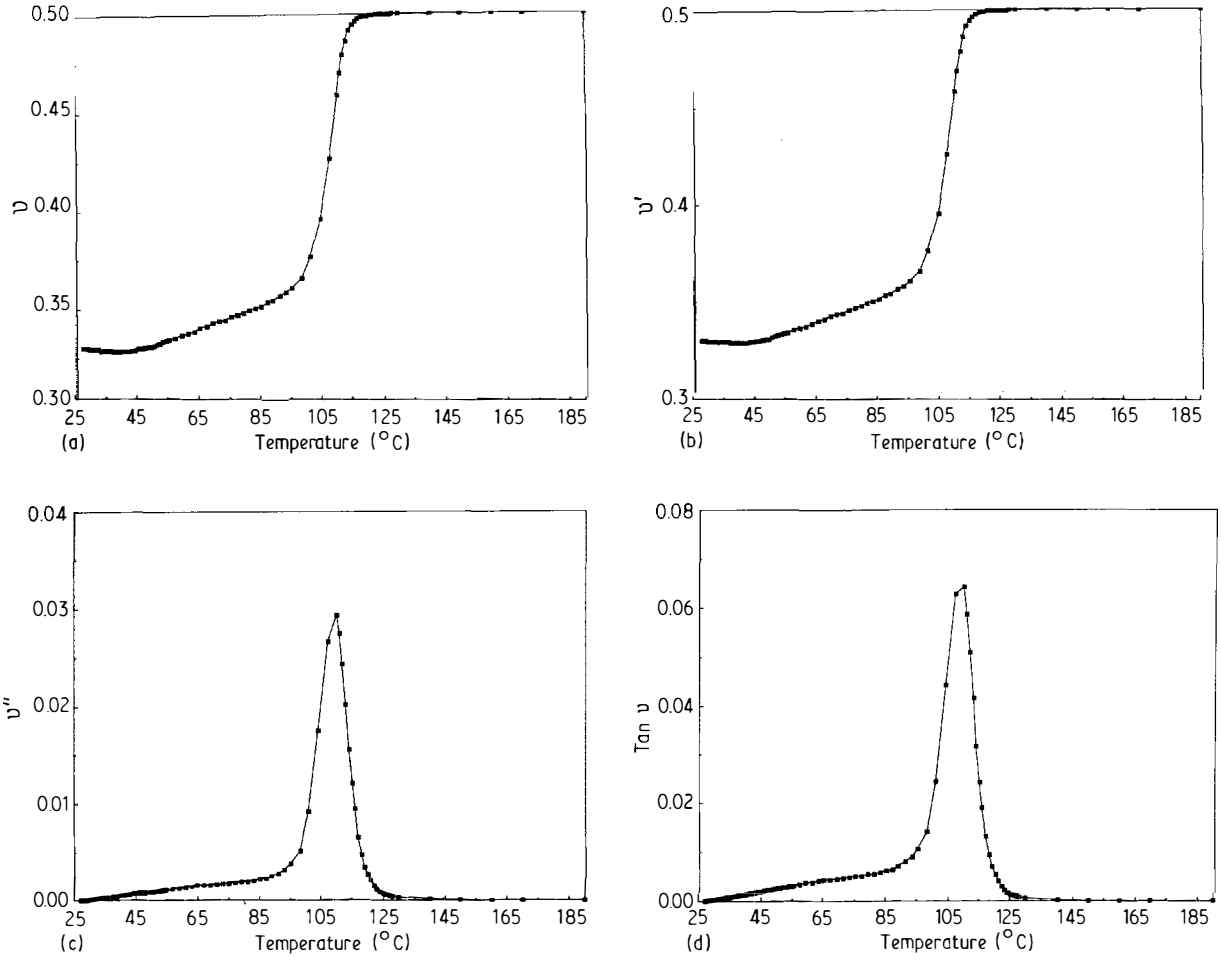

Figure 7 Plots of (a) $\nu_m(= [(\nu'_m)^2 + (\nu''_m)^2]^{1/2})$, (b) ν'_m, (c) ν''_m, and (d) tan ν_m versus temperature for the polystyrene matrix.

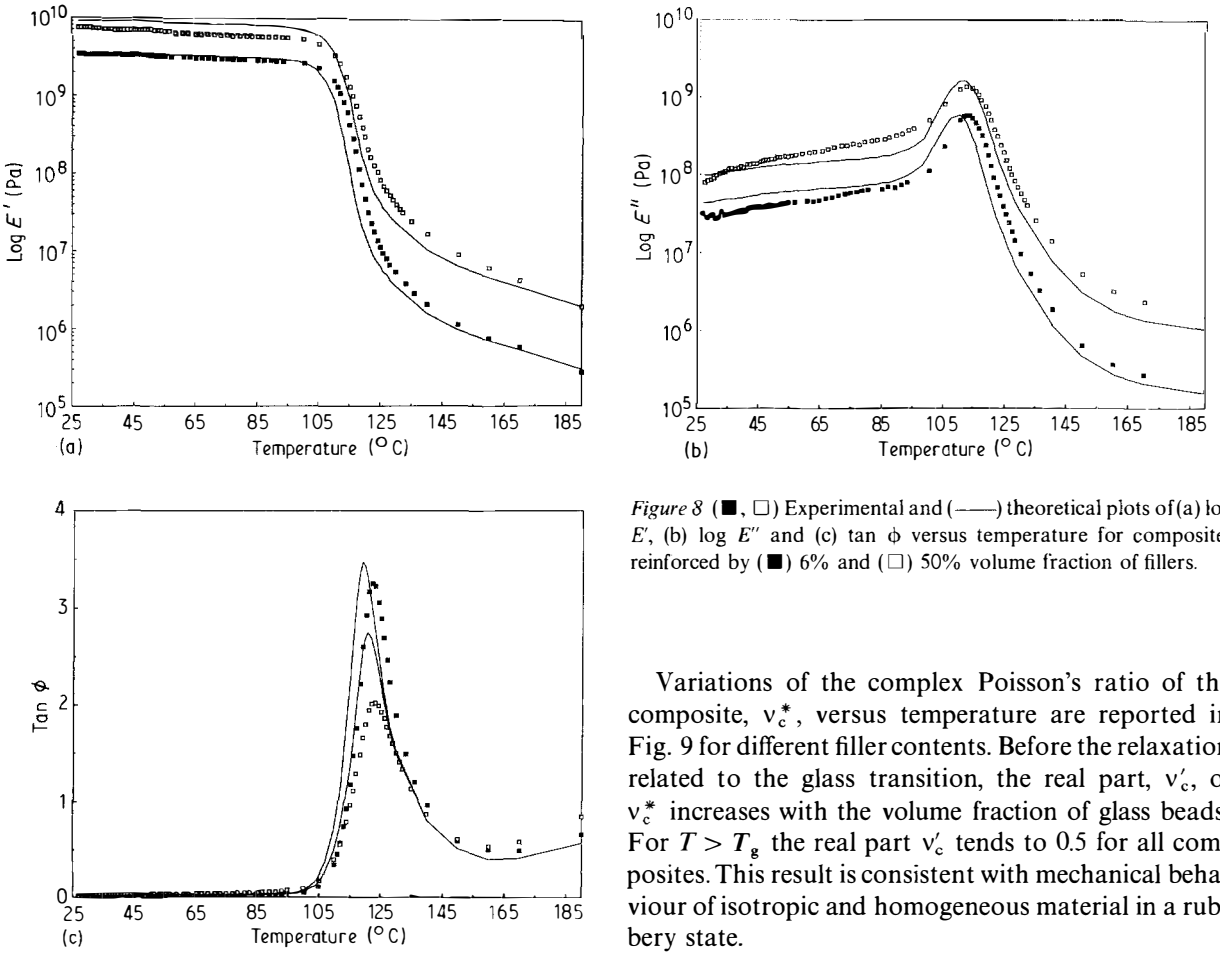

Figure 8 (■, □) Experimental and (——) theoretical plots of (a) log E', (b) log E'' and (c) tan ϕ versus temperature for composites reinforced by (■) 6% and (□) 50% volume fraction of fillers.

Variations of the complex Poisson's ratio of the composite, ν_c^*, versus temperature are reported in Fig. 9 for different filler contents. Before the relaxation related to the glass transition, the real part, ν'_c, of ν_c^* increases with the volume fraction of glass beads. For $T > T_g$ the real part ν'_c tends to 0.5 for all composites. This result is consistent with mechanical behaviour of isotropic and homogeneous material in a rubbery state.

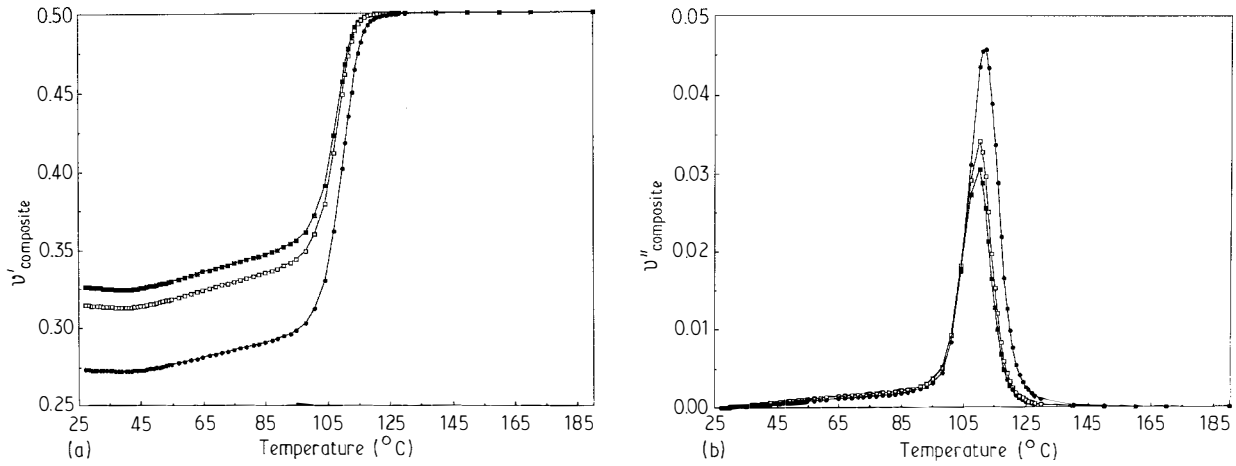

Figure 9 Plots of (a) ν'_c, and (b) ν''_c versus temperature for the different filler contents: (■) 6%, (□) 21% and (●) 50%.

5. Conclusion

Based on experimental analysis of the dynamic mechanical behaviour of polystyrene/glass beads composites, a model of the viscoelastic properties through the glass transition is proposed.

The magnitude of the experimental main relaxation of the composite is significantly reduced on increasing the amount of fillers. A simulation based on Kerner's and Christensen and Lo's models does not furnish evidence for such influence of fillers when considering the Poisson's ratio of the matrix as a real constant over the analysed temperature range. This discrepancy could be related to great differences between the moduli of the two phases, which were enhanced with increasing temperature in the glass transition zone. From these results, it is proposed to consider ν_m as a complex parameter which is time and temperature dependent.

In this paper, a method to evaluate the complex Poisson's ratio of the matrix ν^*_m ($= \nu'_m - i\nu''_m$) has been proposed. Then, theoretical dynamic mechanical behaviour of composites was determined. Therefore, the influence of filler content on the magnitude of the relaxation is taken into account by this numerical simulation. Some differences remain between experimental and theoretical tan ϕ curves for the composite. This could suggest some "interface effects" leading to a reduction in the molecular motion ability of the macromolecular chains

Acknowledgements

This work was financially supported by Composi'tec, by the Rhône Alpes region and by the Research and Technology Ministry (MRT) and we would like to thank J. L. Favre for his help. The contributions of Dr Y. Jayet and of Pr J. Pastor in ultrasonic measurements and in technical advice in program computing, respectively, are also greatly appreciated. The authors are also indebted to Dr P. Cassagnau for preparing the samples.

Appendix

The final solution for G of Christensen and Lo's model is given by the solution of the quadratic Equation 13

$$A\left(\frac{G}{G_m}\right)^2 + 2B\left(\frac{G}{G_m}\right) + C = 0 \qquad (13)$$

where

$$A = 8\left(\frac{G_i}{G_m} - 1\right)(4 - 5\nu_m)\eta_1 v^{10/3} - 2\left[63\left(\frac{G_i}{G_m} - 1\right)\eta_2 + 2\eta_1\eta_3\right]v^{7/3} + 252\left(\frac{G_i}{G_m} - 1\right)\eta_2 v^{5/3} - 50\left(\frac{G_i}{G_m} - 1\right) \times (7 - 12\nu_m + 8\nu_m^2)\eta_2 v + 4(7 - 10\nu_m)\eta_2\eta_3 \qquad (A1)$$

$$B = -2\left(\frac{G_i}{G_m} - 1\right)(1 - 5\nu_m)\eta_1 v^{10/3} + 2\left[63\left(\frac{G_i}{G_m} - 1\right)\eta_2 + 2\eta_1\eta_3\right]v^{7/3} - 252\left(\frac{G_i}{G_m} - 1\right)\eta_2 v^{5/3} + 75\left(\frac{G_i}{G_m} - 1\right) \times (3 - \nu_m)\eta_2\nu_m v + \tfrac{3}{2}(15\nu_m - 7)\eta_2\eta_3 \qquad (A2)$$

$$C = 4\left(\frac{G_i}{G_m} - 1\right)(5\nu_m - 7)\eta_1 v^{10/3} - 2\left[63\left(\frac{G_i}{G_m} - 1\right)\eta_2 + 2\eta_1\eta_3\right]v^{7/3} - 252\left(\frac{G_i}{G_m} - 1\right)\eta_2 v^{5/3} + 25\left(\frac{G_i}{G_m} - 1\right) \times (\nu_m^2 - 7)\eta_2 v - (7 + 5\nu_m)\eta_2\eta_3 \qquad (A3)$$

with

$$\eta_1 = (49 - 50\nu_i\nu_m)\left(\frac{G_i}{G_m} - 1\right) + 35\frac{G_i}{G_m}(\nu_i - 2\nu_m) + 35(2\nu_i - \nu_m) \qquad (A4)$$

$$\eta_2 = 5\nu_i\left(\frac{G_i}{G_m} - 8\right) + 7\left(\frac{G_i}{G_m} + 4\right) \qquad (A5)$$

$$\eta_3 = \frac{G_i}{G_m}(8 - 10\nu_m) + (7 - 5\nu_m) \quad \text{(A6)}$$

and where $\nu_i = (a/b)^3$ is the volume fraction of inclusions.

References

1. Z. HASHIN, *J. Appl. Mech.* **50** (1983) 481.
2. *Idem, ibid.* **29** (1962) 143.
3. R. HILL, *J. Mech. Phys. Solids* **13** (1965) 213.
4. Z. HASHIN and S. SHTRIKMAN, *ibid.* **11** (1962) 127.
5. Z. HASHIN, *Int. J. Solids Struct.* **6** (1970) 539.
6. E. H. KERNER, *Proc. Phys. Soc. Lond.* **69B** (1956) 808.
7. P. S. THEOCARIS, in "The mesophase concept in composites" (Springer-Verlag, Berlin, 1987).
8. M. TAKAYANAGI, K. IMIDA and T. KAJIYAMA, *J. Polym. Sci. C* **15** (1966) 263.
9. J. C. HALPIN and J. L. KARDOS, *J. Appl. Phys.* **43** (1972) 2235.
10. R. A. DICKIE, *J. Appl. Polym. Sci.* **17** (1973) 45.
11. J. D. FERRY, in "Viscoelastic properties of polymers" (Wiley, New York, 1980) p. 558.
12. J. Y. CAVAILLE, C. JOURDAN, J. PEREZ and J. GUILLOT, *Makromol. Chem. Makromol. Symp.* **23** (1989) 411.
13. R. A. DICKIE, *J. Appl. Polym. Sci.* **17** (1973) 65.
14. A. F. YEE and M. T. TAKEMORI, *J. Polym. Sci. Polym. Phys.* **20** (1982) 205.
15. H. A. WATERMAN, *Kolloid Z. Z. Polym.* **192** (1963) 1.
16. *Idem, ibid.* **192** (1963) 9.
17. *Idem, Rheol. Acta* **16** (1977) 31.
18. R. KONO, *J. Phys. Soc. Jpn.* **15** (1960) 718.
19. R. M. CHRISTENSEN and K. H. LO, *J. Mech. Phys. Solids* **27** (1979) 315.
20. J. D. ESHELBY, in "Progress in Solid State Physics," Vol. 3, edited by F. Seitz and D. Turnbull (Academic Press, 1956) p.79.
21. P HEYDEMANN, *Kolloid Z. Z. Polym.* **193** (1963) 12.
22. S. D. SJOERDSMA, A. C. A. M. BLEIJENBERG and D. HEIKENS, *Polymer* **22** (1981) 619.
23. W. J. COUMANS, D. HEIKENS and S. D. SJOERDSMA, *ibid.* **21** (1980) 103.
24. R. KONO, *J. Phys. Soc. Jpn.* **16** (1961) 1793.
25. R. J. CROWSON and R. G. C. ARRIDGE, *Polymer* **20** (1979) 737.
26. J. Y. CAVAILLE, J. PEREZ and G. P. JOHARI, *Phys. Rev. B* **39** (1989) 2411.
27. A. BERGERET, A. AGBOSSOU, N. ALBEROLA, P. C ASSAGNAU and T. SARRAF, *Eur. Polym. J.*, **28** (1992) 1201.